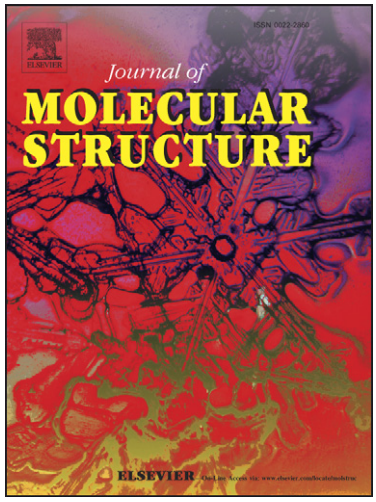

A New Series of Schiff Bases Derived from Sulfa Drugs and Indole-3-carboxaldehyde: Synthesis, Characterization, Spectral and DFT Computational Studies

H. Ebrahimi, J.S. Hadi, H.S. Al-Ansari

PII: S0022-2860(13)00098-7
DOI: http://dx.doi.org/10.1016/j.molstruc.2013.01.063
Reference: MOLSTR 19533

To appear in: *Journal of Molecular Structure*

Received Date: 8 November 2012
Revised Date: 24 January 2013
Accepted Date: 26 January 2013

Please cite this article as: H. Ebrahimi, J.S. Hadi, H.S. Al-Ansari, A New Series of Schiff Bases Derived from Sulfa Drugs and Indole-3-carboxaldehyde: Synthesis, Characterization, Spectral and DFT Computational Studies, *Journal of Molecular Structure* (2013), doi: http://dx.doi.org/10.1016/j.molstruc.2013.01.063

A New Series of Schiff Bases Derived from Sulfa Drugs and Indole-3-carboxaldehyde: Synthesis, Characterization, Spectral and DFT Computational Studies

H. Ebrahimi[1], J. S. Hadi[2,*], H. S. Al-Ansari[2]

[1]Department of Biochemistry and National Magnetic Resonance Facility at Madison (NMRFAM), University of Wisconsin-Madison, Madison, WI 53706, USA

[2]Department of Chemistry, College of Education, University of Basrah, Iraq

Jabbar S. Hadi

Department of Chemistry

University of Basrah

Basrah, Iraq

Tel: (964) 7710822193

*Corresponding Author. E-mail: jshalkabi@yahoo.com

ABSTRACT

A new series of Schiff bases were synthesized for the first time by the condensation of indole-3-carboxaldehyde with various sulfa drugs including sulfanilamide, sulfapyridine, sulfadiazine, sulfamerazine, sulfamethoxazole, sulfamethoxypyridazine and sulfacetamide sodium in ethanol (1:1). The structure of Schiff bases were experimentally characterized by using IR, ^{1}H NMR, ^{13}C NMR and mass spectroscopic methods. The structural and electronic properties of the studied molecules were investigated theoretically by performing density functional theory (DFT) to access reliable results to the experimental values. The molecular geometry, the highest occupied molecular orbital (HOMO), the lowest unoccupied molecular orbital (LUMO) and Mulliken atomic charges of the studied molecules have been calculated at the B3LYP method and standard 6-31+G(d,p) basis set starting from optimized geometry. The theoretical ^{13}C chemical shift results were also calculated using the gauge independent atomic orbital (GIAO) approach and their respective linear correlations were obtained. The comparison of the results indicates that B3LYP/6-31+G(d,p) yields good agreement with the observed chemical shifts.

Keywords: Schiff base, Sulfa drug, Indole-3-carboxaldehyde, ^{13}C NMR, HOMO, DFT computational studies

1. Introduction

Sulfa drugs are known as the first drugs used as preventive and therapeutic compounds against several of bacterial infections such as eye infections, influenza, meningitis and other meningides, actinomices infections, and urinary tract infections [1-3]. They can also be used as model compounds for investigation of mechanisms of the action of drugs [4-6]. A large number of Schiff bases derived from sulpha drugs have been synthesized and used as ligands to prepare potent metal complexes [7-10]. Schiff base compounds have attracted considerable attention in both theoretical and experimental studies. The remarkable electronic and striking tenability of Schiff bases make them to be among the most widely used organic compounds. Schiff bases are applied in many different areas such as catalysts, polymer stabilizers, intermediates in organic synthesis, and as pigments and dyes [11-13]. In addition, Schiff bases are an important class of ligands which are most versatile and thoroughly studied ligands in coordination chemistry. Schiff bases have also been shown to exhibit a broad range of biological activities, including antifungal, antibacterial, antimalarial, anti-proliferative, anti-inflammatory, antiviral, and antipyretic properties [14-16].

In addition, heterocyclic compounds such as indole, pyridine, pyrimidine, pyrazine, and pyridazine as well as related molecules are considered as good ligands because of presence of one nitrogen atom or more which has a localized pair of electrons. For instance, Schiff bases of heterocyclic sulfonamides have been investigated as inhibitors of zinc enzyme carbonic anhydrase as well as management of multitude of tumors [17-19]. These compounds are used in the synthesis of several compounds such as antibiotics, antiallergics, antiphlogistics and antitumor substances [20-22]. The classical synthesis of this important class of compounds goes back to Schiff's report which has involved the condensation of a carbonyl compound with an

amine under azeotropic distillation [23]. The condensation products of sulfa drugs with aldehydes, ketones or their derivatives are very active biologically, besides having good complex ability [24].

Also, prediction of molecular properties of polyatomic molecules by quantum mechanical methods has become important because of its accurate and consistent with experimental data. By increasing development of computational chemistry, density functional theory (DFT) has been extensively used to calculate a wide variety of molecular properties and provided reliable results which are in accordance with experimental data [25, 26].

In connection of widely applications for this major class of compounds, for the first time, we have synthesized and characterized a new series of Schiff bases derived from sulfa drugs and indole-3-carboxaldehyde. Also, these new synthesized compounds have been characterized on the basis of spectroscopic methods including IR, ^{1}H and ^{13}C NMR as well as mass spectroscopy. To additionally verify the proposed assignments, quantum chemical calculations have been performed. In the present study, we have also extended the probing into the application of DFT methods. Therefore, these synthesized compounds have theoretically investigated by using the more popular DFT methods, B3LYP, in 6-31+G(d,p) basis set. In order to make sense between the experimental and theoretical results, the electronic properties such as HOMO-LUMO energies, and Mulliken atomic charges were calculated and the results were discussed.

2. Experimental procedure

2.1. Materials

All of the chemicals and solvents employed in synthesis were of extra-pure grade and used as received without further purification. Sulfanilamide, sulfapyridine, sulfadiazine, sulfamerazine, sulfamethoxazole, sulfamethoxypyridazine and sulfacetamide sodium as well as indole-3-carboxaldehyde were obtained from Fluka and Himedia. The organic solvents used included absolute ethanol and ethyl acetate were obtained from BDH and Riedel-de haen.

2.2. Instrumentation and spectral measurements

IR spectra were recorded by using Shimadzu FTIR-8300 spectrophotometer in the region 4000-200 cm^{-1} in KBr pellet and in CCl_4 solution. The spectra were collected with a resolution of 2 cm^{-1} with 15 scans. The experimental values of ^{1}H and ^{13}C NMR as well as DEPT-135 spectra for the studied compounds were scanned on a Bruker Avance DX500 MHz spectrometer with a field gradient operating at 500.13 MHz for proton observation. TMS as the internal standard was used as referenced to 0.0 ppm. DMSO-d_6, D_2O, CD_3OD were used as solvents. The experiments were run in unlock mode, with sufficient a number of scans to achieve S/N ratios 200:1 (ca.). NMR spectra were obtained at a probe temperature of about 298 K. Melting points were determined using a BUCHI 510 apparatus in open capillaries and were left uncorrected. The mass spectra were scanned by the EI technique at 70 eV with an Agilent Technologies 5975C spectrometer.

2.3. Synthesis of Schiff Base Compounds

2.3.1. Preparation of ISN, ISD, ISM, ISMT, ISMP, ISPY and ISA

The title compounds were synthesized in a general procedure by the condensation of Indole-3-carboxaldehyde with sulfanilamide, sulfadiazine,

sulfamerazine, sulfamethoxazole, sulfamethoxypyridazine, sulfapyridine and sulfacetamide sodium, respectively, in ethanol (1:1). The synthesis of Schiff bases were performed in accordance with reaction Scheme 1. The reaction mixture was refluxed for half to three hours and allowed to cool, filtered and the products recrystallized by appropriate solvent. The purity of the products and composition of the reaction mixture were monitored by thin layer chromatography using chloroform: ethanol (9:1) or ethyl acetate: benzene (3:7). The structures of synthesized Schiff bases with related sulfa drugs are shown in Table 1. Also, the observed physical properties of title compounds are given in Table 2.

3. Computational aspects

In present work, a non-local DFT method, B3LYP, was used to perform theoretical calculations on the studied compounds. The DFT methods are more advantageous owing to their accuracy and low computational cost. These properties make DFT more practical and feasible for the computations of different molecules [27-30]. As the more popular DFT methods, B3LYP is consistently one of the best performing DFT methods. The geometry of all compounds was fully optimized at the B3LYP level of theory along with standard 6-311+G(d,p) basis set which has amply been proven to give very good ground-state geometries. Vibrational frequency analyzes, calculated at the same level of theory, indicate that the optimized structures are at the stationary points corresponding to local minima without any imaginary frequency. The electronic properties were calculated using B3LYP method based on the optimized structures. In addition, a comparison was made between the theoretically calculated ^{13}C chemical shift constants and the experimentally measured ^{13}C chemical shifts. GIAO (Gauge Including Atomic Orbital) as the most widely used

approach for calculating NMR shielding tensors were applied [31-35]. The Gaussian 09 package was employed to perform optimization of structures and all the calculations [36].

4. Results and discussion

4.1. Experimental results

In this section, spectral studies including the observed spectroscopic results for the title compounds are discussed.

4.1.1. IR spectra analysis

The infrared spectral data of the studied compounds are listed in Table 3. IR spectra of compounds showed a strong band at 1653–1636cm^{-1} that attributed to azomethine ν(CH=N). The absence of band ~1720 and 3300 cm^{-1} due to carbonyl stretching and NH_2 stretching respectively indicates the condensation of indole-3-carboxaldehyde and sulfa drugs in 1:1 mole ratio. The high value of ν(CH=N) stretching in these compounds when compared with that derived from another aromatic aldehyde (substituted benzaldehyde, naphthaldehyde, etc.) can be explained by a strain of indole moiety. All IR spectra of compounds show a first strong band within the range 1376–1228cm^{-1} which attributed to asymmetric stretching of (O=S=O) and the second within the range 1163–1136 assigned to symmetric stretching of (O=S=O) [37].

4.1.2. Mass spectra analysis

All compounds show a molecular ion ($M^{\cdot+}$) with low relative intensity except **ISN** (40%). The molecular ion peaks are in agreement with proposed empirical formulas. The loss of 64 units (SO_2 group) generates an intense peak in most

compounds spectra where this peak represents the base peak. The possible suggested ion fragments as the result of fragmentation of the **ISN** is given in Scheme 2. The important fragments and their intensity for the other molecules are given in Table 4.

4.1.3. ^{1}H and ^{13}C NMR spectra analysis

^{1}H NMR spectra recorded in different solvents namely in DMSO-d_6 as well as DMSO-d_6 + D_2O or in CD_3OD. The ^{1}H NMR spectrum of **ISM** with and without D_2O is presented in Fig. 1. The spectra of all compounds show the azomethine proton (CH=N) as singlet signal at δ ~ 9.86–9.93 ppm in all solvents. The ^{1}H NMR spectra of **ISN**, **ISM**, and **ISMT** display the NH of indole moiety as singlet signal at ~12 (in DMSO-d_6), while the signal cannot be seen in their spectra due to deuterium exchange in DMSO-d_6+D_2O. The signal of NH proton in sulfa moiety appears as singlet at ~6 ppm in case of compounds **ISM** and **ISMT** disappear after addition of D_2O (Fig. 1). As expected, the NH proton of sulfa moiety shows different chemical shifts when the spectra recorded in CD_3OD where the signal appears at ~8.3 as a broad signal in **ISMP** and **ISA** compounds. The chemical shifts of different types of protons in all compounds are listed in Table 5.

The ^{13}C NMR spectra and DEPT-135 of compounds were recorded in DMSO-d_6. All spectra exhibited signals from azomethine carbon at δ=184 ppm as the highest chemical shift in our synthesized Schiff bases. All quaternary carbon atom signals disappear in DEPT-135. The measured chemical shifts of all carbon atoms for **ISN**, **ISM** and **ISMT** are listed in Table 6, where the numbering of the carbon atoms is presented only for ^{13}C NMR data assignment in Fig. 2. Also, magnetically equivalent carbons are displayed by same number.

4.2. Computational results

As mentioned above, all calculation carried out in B3LYP method in 6-31+G(d,p) basis set. The results are discussed for **ISMT** as a case study and results for other Schiff bases are given in supplementary data. The optimized structure of **ISMT** along with labeling of atoms is shown in Fig. 3. The figure shows the molecule in the ball and stick model. The geometry optimization yields non planar structure. Also, the most optimized structural parameters of **ISMT** calculated by B3LYP/6-311+G(d,p) are presented in Table 7.

4.2.1. Electronic properties

The most important orbitals in a molecule are the frontier molecular orbitals, called HOMO (the highest occupied molecular orbital) and LUMO (the lowest-lying unoccupied molecular orbitals). The HOMO represents the ability to donate an electron, LUMO as an electron acceptor represents the ability to obtain an electron. These orbitals play an important role in the electric properties and determine the way the molecule interacts with other species [38-40]. Both the HOMO and the LUMO are the main orbital taking part in chemical reaction. While the energy of the HOMO is directly related to the ionization potential, LUMO energy is directly related to the electron affinity. Also, the frontier orbital gap, the energy gap between HOMO and LUMO, represents stability of structures and helps to characterize some significant issues including the kinetic stability as well as chemical reactivity of the molecule [41]**.** A molecule with a small frontier orbital gap is more polarizable and is generally associated with a high chemical reactivity as well as low kinetic stability [42]. The conjugated molecules are characterized by a small highest occupied molecular orbital-lowest unoccupied molecular orbital (HOMO-LUMO) separation.

In order to evaluate the energetic behavior of the title compounds, we carried out calculations for **ISMT**. The HOMO and LUMO energy calculated by B3LYP method in 6-31+G(d,p) basis set is presented in Table 8. The plots of frontier molecular orbitals for **ISMT** are shown in Fig. 4. It is clear from the figure that, while the HOMO is localized on whole the indole and almost the benzene ring, the LUMO is localized mainly on the indole, the benzene ring and oxygen atoms in sulfonyl group. These orbitals significantly overlap in their position over the indole ring. The frontier energy gap implies an electron density transfer to the benzene ring from the indole ring and also explains the eventual charge transfer occurs within the compound. According to calculation, the energy band gap of **ISMT** reveals about -0.37 a.u. by B3LYP method at the mentioned basis set. The detail result in B3LYP is

HOMO energy = -0.293 a.u.

LUMO energy = 0.078 a.u.

HOMO-LUMO energy gap = -0.37 a.u.

This small energy gap confirms the conjugated compound with high chemical reactivity as well as high polarizability.

4.2.2. Mulliken population analysis

The Mulliken analysis is the most common population analysis method. Mulliken atomic charge calculation has a significant role in the application of quantum chemical calculations to molecular systems because of atomic charges affect some properties of molecular systems including dipole moment, and molecular polarizability. It also has been used to describe the electrostatic potential surfaces [43-45]. The total atomic charge values of **ISMT** obtained by Mulliken population

analysis [46] in the applied method are listed in Table 9. The charge changes with methods presumably occur due to variation of the hybrid functionals. Illustration of atomic charges plotted is shown in Fig. 5. As can be seen in Table 9 and Fig. 5, all the hydrogen atoms have a net positive charge. The obtained atomic charge shows that the H5 atom has bigger positive atomic charge (0.3384e) than the other hydrogen atoms. This is due to the presence of electronegative nitrogen atom (N4), the hydrogen atom (H5) attracts the positive charge from the nitrogen atom (N4). Moreover, Mulliken atomic charges also confirm that an H38 atom in indole ring is more acidic due to more positive charge. As expected, the results show that the charge of the nitrogen atom (N26) in imine group and the charge of the nitrogen atom in indole ring, the charge of N43, are negative. Considering the applied method used in the atomic charge calculation, the oxygen atoms in sulfonyl group exhibit a negative charge, which are donor atoms.

4.2.3. NMR analysis

In order to comparison between experimental and theoretical NMR data, which may be helpful in making correct assignments and understanding the relationship between chemical shift and molecular structure, ^{13}C NMR chemical shifts calculation for further clarification of synthesized molecules are reported. To clarify the relation between theoretical and experimental values of NMR chemical shift constants, the experimental data are plotted versus computed values.

The ^{13}C NMR chemical shifts of all carbons were calculated on the optimized structures of compounds using B3LYP method employing 6-31+G(d,p) basis set for all atoms. The impact of the solvent was taken into account using the Polarized Continuum Model (PCM) of Tomasi et al. [47]. In order to compute the ^{13}C NMR chemical shifts, each couple of carbon atoms on equivalent locations of the molecule

were considered as equivalent and their average of chemical shifts were calculated. The isotropic ^{13}C chemical shifts for other compounds are given in supplementary data and compared with the experimental values. The statistical parameters of computed ^{13}C NMR chemical shifts at the B3LYP/6-31+G(d,p) level of theory along with experimental data for **ISN**, **ISM**, and **ISMT** compounds are given in Table 10. As can be seen, the results obtained by using this method are in reasonable agreement with experimental values. The results are close to experimental data and they differ slightly from results of experiment. As shown in Fig. 6, there is a good linear relationship between experimental and theoretical B3LYP/6-31+G(d,p) chemical shifts. Similar plots for other calculated NMR results are given in supplementary content.

5. Conclusion

The synthesis, characterization, and theoretical study of several new Schiff bases derived from condensation of sulfa drugs and Indole-3-carboxaldehyde were reported. Spectroscopic techniques including IR, ^{1}H and ^{13}C NMR, and mass analysis were used to identify the products. To study the structural and electronic properties of studied molecules, complete analyses of the ^{13}C NMR spectra, HOMO-LUMO energy gap as well as the Mulliken atomic charges of title compounds was reported. All theoretical calculations were carried out by the more popular DFT methods, B3LYP, at 6-31+G(d,p) level of theory. The applied method is in good accordance with experimental values. The HOMO-LUMO energy gap as an important value for stability index revealed high chemical reactivity of synthesized compounds in chemical reactions.

Supplementary data

Supplementary data contains a complete set of experimental and theoretical ^{13}C chemical shifts with related plots.

References

[1] M.K. Yun, Y. Wu, Z. Li, Y. Zhao, M.B. Waddell, A.M. Ferreira, R.E. Lee, D. Bashford, S.W. White, Science 335 (2012) 1110-14.

[2] P. Nagpal, R.V. Singh, Appl. Organometal. Chem. 18 (2004) 221-226.

[3] A. Scozzafava, T. Owa, A. Mastrolorenzo, C.T. Supuran, Curr. Med. Chem. 10 (2003) 925-953.

[4] A.M. Tawfik, M.A. El-ghamry, S.M. Abu-El-Wafa, N.M. Ahmed, Spectrochim. Acta A 97 (2012) 1172-1180.

[5] M.A. Halim, D.M. Shaw, R.A. Poirier, J. Mol. Struct.: THEOCHEM 960 (2010) 63-72.

[6] W.C. Cutting, Handbook of Pharmacology, third ed., Meredith, New York, 1967.

[7] G.G. Mohamed, C.M. Sharaby, Spectrochim. Acta A 66 (2007) 949-958

[8] A.M. Mansour, J. Mol. Struct. 1035 (2013) 114-123.

[9] R.C. Maurya, S. Rajput, J. Mol. Struct. 794 (2006) 24-34.

[10] C. Topacli, A. Topacli, J. Mol. Struct. 654 (2003) 131-137.

[11] G. Gümrükçü, G.K. Karaoglan, A. Erdogmus, A. Gül, U. Avcıata, Dyes and Pigments 95 (2012) 280-289.

[12] K.C. Gupta, A.K. Sutar, C.C. Lin, Coor. Chem. Rev. 253 (2009) 1926-1946.

[13] D. Lorcya, N. Belleca, M. Fourmiguea, N. Avarvari, Coor. Chem. Rev. 253 (2009) 1398-1438.

[14] M.A. Ashraf, K. Mahmood, A. Wajid, International Conference on Chemistry and Chemical Process. IPCBEE, Singapore, 10 (2011) 1-7.

[15] P. Przybylski, A. Huczynski, K. Pyta, B. Brzezinski, F. Bartl. Curr. Org. Chem. 13 (2009) 124-148.

[16] S.N. Pandeya, D. Sriram, G. Nath, E. DeClercq, Eur. J. Pharma. Sci. 9 (1999) 25-31.

[17] M.H. Ul, Z.H. Chohan, A. Scozzafava, C.T. Supuran, J. Enz. Inhib. Med. Chem. 19 (2004) 263-267.

[18] A. Popescu, A. Simion, A. Scozzafava, F. Briganti, C.T. Supuran, J. Enz. Inhib. Med. Chem. 14 (1999) 407-423.

[19] C.T. Supuran, A. Nicolae, A. Popescu, Eur. J. Med. Chem. 31 (1996) 431-438.

[20] D. Barton, W.D. Ollis, Comprehensive Organic Chemistry, Vol. 2, Pergamon, Oxford, 1979.

[21] R.W. Layer, Chem. Rev. 63 (1963) 487-510.

[22] C.K. Ingold, Structure and Mechanism in Organic Chemistry, Second ed., Cornell Uni., Ithaca, 1969.

[23] R.B. Moffett, in: Rabjohn N (editor), Organic syntheses, Vol.4. John Wiley & Sons, Inc., New York, 1963. p. 605-608.

[24] H.L. Singh, S. Varshney, A.K. Varshney, Appl. Organometal. Chem. 14 (2000) 212-217.

[25] M. Buhl, T.V. Mourik. WIREs. Comput. Mol. Sci. 1 (2011) 634-647.

[26] W. Koch, M.C. Holthausen, A Chemist's Guide to Density Functional Theory, Second ed., WILEY, Weinheim, 2001.

[27] M. W. Lodewyk, M.R. Siebert, D.J. Tantillo, Chem. Rev. 112 (2012) 1832-1869.

[28] M. Kaoupp, M. Bühl, V. G Malkin, Calculation of NMR and EPR Parameters: Theory and Applications, Wiley, New York, 2004.

[29] H. Shaghaghi, H. Ebrahimi, N. Bahrami Panah, M. Tafazzoli, Solid State Nucl. Magn. Reson. 49-50 (2013).

[30] H. Shaghaghi, H. Ebrahimi, F. Fathi, M. Tafazzoli, Conc. Mag. Reson. A 42 (2013).

[31] H. Ebrahimi, M. Tafazzoli, Conc. Mag. Reson. A 40 (2012) 192-204.

[32] H. Ebrahimi, H. Shaghaghi, M. Tafazzoli, Conc. Mag. Reson. A 38 (2011) 269-279.

[33] M. Tafazzoli, H. Ebrahimi, Phosphorus, Sulfur, Silicon Related Element 186 (2011) 1491-1500.

[34] H. Ebrahimi, H. Shaghaghi, M. Tafazzoli, M. Jalali-Heravi, J. Fluorine Chem. 131 (2010) 47-52.

[35] S. G. Smith, J. M. Goodman, J. Org. Chem. 74 (2009) 4597-4607.

[36] M.J. Frisch, G.W. Trucks, H.B. Schlegel, G.E. Scuseria, M.A. Robb, J.R. Cheeseman, G. Scalmani, V. Barone, B. Mennucci, G. A. Petersson, H. Nakatsuji, M. Caricato, X. Li, H. P. Hratchian, A. F. Izmaylov, J. Bloino, G. Zheng, J. L. Sonnenberg, M. Hada, M. Ehara, K. Toyota, R. Fukuda, J. Hasegawa, M. Ishida, T. Nakajima, Y. Honda, O. Kitao, H. Nakai, T. Vreven, J. A. Montgomery, Jr., J. E. Peralta, F. Ogliaro, M. Bearpark, J. J. Heyd, E. Brothers, K. N. Kudin, V. N. Staroverov, R. Kobayashi, J. Normand, K. Raghavachari, A. Rendell, J. C. Burant, S. S. Iyengar, J. Tomasi, M. Cossi, N. Rega, J. M. Millam, M. Klene, J. E. Knox, J. B. Cross, V. Bakken, C. Adamo, J. Jaramillo, R. Gomperts, R. E. Stratmann, O. Yazyev, A. J. Austin, R. Cammi, C. Pomelli, J. W. Ochterski, R. L. Martin, K. Morokuma, V. G. Zakrzewski, G. A. Voth, P. Salvador, J. J. Dannenberg, S. Dapprich, A.D. Daniels, Ö. Farkas, J.B. Foresman, J.V. Ortiz, J. Cioslowski, and D.J. Fox, Gaussian 09, Revision A.1, Gaussian, Inc., Wallingford CT, 2009.

[37] G. Socrates, Infrared characteristic group frequencies, John Wiley, New York, 1994.

[38] M. Govindarajan, S. Periandy, K. Carthigayen, Spectrochim. Acta A 97 (2012) 411-422.

[39] M. Govindarajan, M. Karabacak, Spectrochim. Acta A 96 (2012) 421-435.

[40] C. Ravikumar, I.H. Joe, V.S. Jayakumar, Chem. Phys. Lett. 460 (2008) 552-558.

[41] L.A. Curtiss, P.C. Redfern, K. Raghavachari, J.A. Pople, J. Chem. Phys. 42 (1998) 117-122.

[42] I. Fleming, Frontier Orbitals and Organic Chemical Reactions, John Wiley & Sons, New York, 1976.

[43] V. Balachandran, K. Parimala, Spectrochim. Acta A 96 (2012) 340-351.

[44] A. Lakshmi, V. Balachandran, J. Mol. Struct. 1033 (2013) 40-50.

[45] S. Ramalingama, M. Karabacak, S. Periandy, N. Puviarasan, D. Tanuja, Spectrochim. Acta A 96 (2012) 207-212.

[46] R.S. Mulliken, J. Chem. Phys. 23 (1955) 1833-1840.

[47] V. Barone, M. Cossi, J. Tomasi, J. Chem. Phys. 107 (1997) 3210-3221.

Table 1. Structures of synthesized Schiff bases with related sulfa drugs

Schiff base structure	Sulfa drug	Schiff base
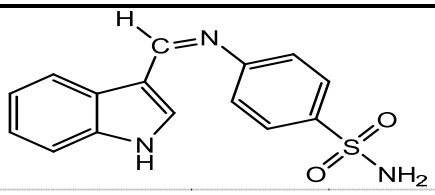	Sulfanilamide	**ISN**
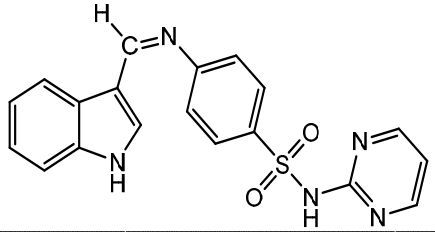	Sulfadiazine	**ISD**
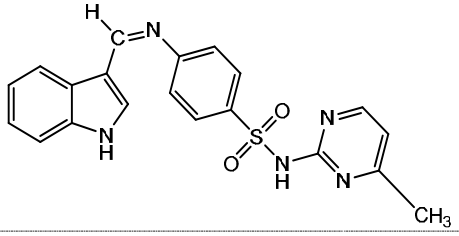	Sulfamerazine	**ISM**
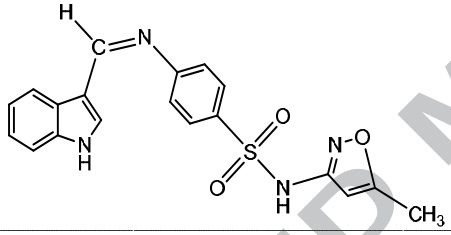	Sulfamethoxazole	**ISMT**
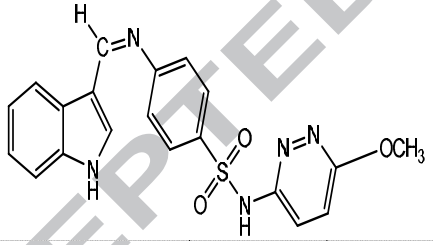	Sulfamethoxypyridazine	**ISMP**
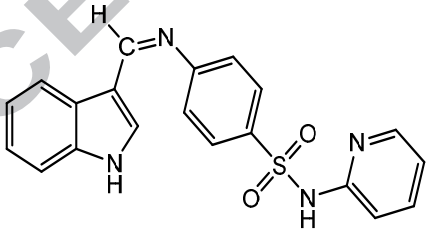	Sulfapyridine	**ISPY**
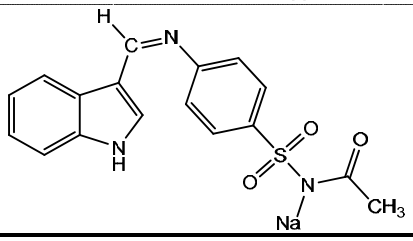	Sulfacetamide sodium	**ISA**

Table 2. Physical properties of studied compounds

Yield %	Reaction time (min)	Solvent of Recrystallization	Color, melting point (°C)	MW, Physical state	Molecular Formula	Compound
40	30	Ethanol	O (224-227)	299.2 (s)	$C_{15}H_{13}N_3O_2S$	**ISN**
80	120	Ethanol	O-Y (218-220)	377.3 (c)	$C_{19}H_{15}N_5O_2S$	**ISD**
44	90	Ethanol	O-Y (162-164)	391.4 (c)	$C_{20}H_{17}N_5O_2S$	**ISM**
21	120	Water: Ethanol 1:1	O (178-180)	380.4 (s)	$C_{19}H_{16}N_4O_3S$	**ISMT**
37	20	Ethanol	Y (236-238)	407.4 (c)	$C_{20}H_{17}N_5O_3S$	**ISMP**
35	120	Dichloro-methane	Y (147-150)	376.4 (s)	$C_{20}H_{16}N_4O_2S$	**ISPY**
72	60	Ethanol	Y (168-170)	363.3 (s)	$C_{17}H_{14}N_3NaO_3S$	**ISA**

s: Solid, c: Crystal, O: Orange, O-Y: Orange-Yellowish, Y: Yellow

Table 3. IR spectral data with vibrational assignment of the studied compounds

Bond	N-H		C=C	C-H			C=N	O=S=O	Other
Compound	Indole 3-Aldehyde	Sulfa	Aromatic	Azomethine	Sp^2	Sp^3	Azomethine	Asy[a]/Sym[b]	
ISN	3240	3477Asy 3418Sym	1500	2925	3100 Asy 3050 Sym	—	1649	1342 Asy 1155 Sym	1558(s) (NH bend)
ISD	3252	3348	1493	2934	3109 Asy 3078 Sym	—	1653	1338 Asy 1153 Sym	1585(s) (NH bend)
ISM	3171	3385	1445	2928	3107 Asy 3043 Sym	2860 Asy 2820 Sym	1636	1331 Asy 1 148 Sym	1518(m) (NH bend)
ISMT	3171	3456	1447	2976	3105 Asy 3042 Sym	2930 Asy 2900 Sym	1636	1387 Asy 1128 Sym	1524(m) (NH bend)
ISMP	3210	3448	1491	2922	3188 Asy 3096 Sym	2858 Asy 2818 Sym	1653	1342 Asy 1128 Sym	1579(s) (NH bend)
ISPY	3240	3369	1447	2930	3103 Asy 3043 Sym	—	1636	1387 Asy 1132 Sym	1518(m) (NH bend)
ISA	3286	—	1491	2983	3150 Asy 3067Sym	2930 Asy 2856 Sym	1649	1336 Asy 1155 Sym	1709 (C=O) 1583(s) (NH bend)

[a] Asymmetry, [b] Symmetry

Table 4. The mass spectra data of the studied compounds

Compound	*m/z* (%)
ISN	$M^{\cdot+}$ 299.1 (40), $[M-SO_2]^{\cdot+}$ 235 (8), 219 (18), 172 (97), 156 (base peak), 143 (10), 116 (11).
ISD	$M^{\cdot+}$ 377 (1), $[M-SO_2]^{\cdot+}$ 313 (6), 185 (base peak), 156 (3), 108 (18), 92 (35).
ISM	$M^{\cdot+}$ 391 (3), 299 (8), 199 (43), 146 (80), 144 (base peak), 116 (39), 89 (33).
ISMP	$M^{\cdot+}$ 409 (3), $[M-SO_2]^{\cdot+}$ 343 (15), 339 (20), 312 (5), 245 (35), 215 (12), 171 (base peak), 115(13), 92 (8).
ISPY	$M^{\cdot+}$ 377 (1), 312 (8), 184 (base peak), 170 (3), 153 (6), 108 (19), 92 (41), 85 (29).
ISA	$M^{\cdot+}$ 363 (3), 348 (4), 320 (4), 299 (base peak), 265 (9), 235(16), 208 (46), 156 (49), 108 (51), 92 (66), 83 (69).

Table 5. ^{1}H NMR chemical shifts (in ppm)

OCH_3	SO_2NH_2	Methyl	CH=N	NH		H (aromatic)	Compound
				(Indole moiety)	(Sulfa moiety)	(Ar–H)	
---	6.9	---	9.93	12.1 (s)	---	6.6-8.59, 9H (m)	**ISN**
---	---	---	9.32	12.31 (s)	8.2 (br)	7.0-8.48, 12H (m)	**ISD**
---	---	2.3	9.93	12.0 (s)	6.0 (s)	6.7-8.3, 10H (m)	**ISM**
---	---	1.05	9.86	12.2 (s)	6.0 (s)	7.2-8.2, 10H (m)	**ISMT**
3.9	---	---	9.87	9.4 (br)	8.35 (br)	6.6-8.1, 11H (m)	**ISMP**
---	---		9.86	8.1 (br)	6.9 (br)	6.6-8.4, 13H (m)	**ISPY**
---	---	1.92	9.90	8.3 (br)	---	7.2-8.7, 9H (m)	**ISA**

s: singlet, d: doublet, m: multiplet, br: broad

Table 6. ^{13}C chemical shifts (in ppm) for **ISN**, **ISM** and **ISMT**

ISMT		**ISM**		**ISN**		
DEPT	Exp.	DEPT	Exp.	DEPT[b]	Exp.	Carbon[a]
185.4	185.4	185.4	185.4	185.4	185.4	1
---	118.6	---	118.6	---	118.6	2
---	124.6	---	124.6	---	124.5	3
123.9	123.9	123.9	123.9	123.9	123.9	4
122.6	122.6	122.6	122.6	122.6	122.6	5
123.9	123.9	123.9	123.9	123.9	123.9	6
121.2	121.2	121.3	121.3	121.3	121.3	7
---	130.3	---	130.5	---	130.5	8
138.9	138.9	138.9	138.9	138.9	138.9	9
---	151.9	---	153.4	---	152.3	10
112.8	112.8	112.8	112.8	112.9	112.9	11
126.5	126.5	130.5	130.5	127.9	127.9	12
---	137.5	---	137.5	---	137.5	13
---	151.9	---	157.4			14
---	170.3	138.9	138.9			15
12.5	12.5	121.3	121.3			16
97.6	97.6	---	153.4			17

[a] Labeling numbers are given in Fig. 2.
[b] DEPT: Distortionless Enhancement by Polarization Transfer spectrum

Table 7. Optimized geometrical parameters of **ISMT** calculated by B3LYP/6-311+G(d,p)

Value (°)	Dihedral angle	Value (°)	Bond angle	Value (Å)	Bond length
170.0	O2–S1–N4–H5	122.7	O2–S1–O3	1.464	S1–O2
-49.8	O2–S1–N4–C6	105.8	O2–S1–N4	1.463	S1–O3
-159.0	O2–S1–C16–C17	103.3	O3–S1–N4	1.708	S1–N4
22.3	O2–S1–C16–C18	111.4	H5–N4–S1	1.788	S1–C16
39.8	O3–S1–N4–H5	122.7	C6–N4–S1	1.017	N4–H5
179.9	O3–S1–N4–C6	113.7	C6–N4–H5	1.398	N4–C6
-23.8	O3–S1–C16–C17	103.3	C6–C7–C9	1.426	C6–C7
157.5	O3–S1–C16–C18	127.4	C6–C7–H10	1.317	C6–N11
-175.2	N4–C6–N11–O8	104.7	C6–N11–O8	1.363	C7–C9
2.986	H5–N4–C6–N11	109.7	C7–C9–O8	1.077	C7–H10
178.7	O8–C9–C7–H10	109.4	C9–O8–N11	1.353	C9–O8
-1.319	C16–C17–C19–C23	110.7	C9–C12–H13	1.488	C9–C12
0.064	C16–C18–C21–C23	110.8	C9–C12–H14	1.115	N11–O8
179.3	C17–C19–C23–N26	110.0	C9–C12–H15	1.095	C12–H13
-178.5	C18–C21–C23–N26	107.7	H13–C12–H14	1.095	C12–H14
0.045	C19–C17–C16–C18	108.6	H13–C12–H15	1.091	C12–H15
-179.0	H20–C17–C16–C18	108.7	H14–C12–H15	1.401	C16–C17
-179.2	H24–C19–C23–C21	108.1	C16–S1–O2	1.397	C16–C18
-0.161	H25–C21–C23–N26	108.3	C16–S1–O3	1.389	C17–C19
-178.7	H25–C27–H28–C29	119.9	C16–C17–H20	1.084	C17–H20
177.4	N26–C23–C19–C21	120.1	C16–C18–H22	1.392	C18–C21
-2.274	N26–C27–C29–C30	120.7	C17–C19–C23	1.084	C18–H22
177.7	N26–C27–C29–C31	120.6	C18–C21–C23	1.409	C19–C23
-179.9	C27–C29–C30–C32	119.7	C23–N26–C27	1.085	C19–H24
-0.078	C27–C29–C30–C33	120.9	N26–C27–H28	1.409	C21–C23
179.9	C27–C29–C31–N43	123.3	N26–C27–C29	1.085	C21–H25
178.9	H28–C27–C29–C30	106.7	C29–C30–C32	1.398	C23–N26
179.1	H28–C27–C29–C31	109.7	C29–C31–N43	1.289	C27–N26
179.9	C29–C30–C32–C35	106.4	C30–C29–C31	1.100	C27–H28
-179.9	C29–C30–C33–C36	122.6	C30–C32–C35	1.440	C27–C29
0.019	C29–C30–C32–N43	107.3	C30–C32–N43	1.450	C30–C29
0.021	C29–C31–N43–C32	109.5	C31–N43–C32	1.418	C30–C32
-0.019	C30–C32–C35–C39	125.0	C31–N43–H38	1.405	C30–C33
0.014	C30–C33–C36–C39	117.1	C32–C35–C39	1.081	C31–H34
-0.025	C31–N43–C32–C30	121.3	C33–C36–C39	1.367	C31–N43
-179.9	C31–N43–C32–C35	120.9	H34–C31–N43	1.397	C32–C35
-0.015	C32–C35–C39–C36	129.9	C35–C32–N43	1.392	C33–C36
0.017	C33–C36–C39–C35	121.1	C35–C39–C36	1.392	C35–C39
0.096	H34–C31–N43–H38	119.3	C35–C39–H42	1.410	C36–C39
-0.007	H37–C33–C36–H41	119.4	C36–C39–H42	1.390	N43–C32
-0.004	H42–C39–C35–H40	119.1	C39–C36–H41	1.008	N43–H38

Table 8. HOMO-LUMO energy values of **ISMT**

Energy (a.u.)	
-0.2929	HOMO
-0.0778	LUMO
-0.3707	HOMO-LUMO energy gap

Table 9. Mulliken atomic charge of **ISMT**

Charge	Atom	Charge	Atom	Charge	Atom	Charge	Atom
0.1475	34 H	-0.5799	23 C	-0.6963	12 C	1.4039	1 S
0.0490	35 C	0.1385	24 H	0.1798	13 H	-0.5074	2 O
-0.3341	36 C	0.1254	25 H	0.1781	14 H	-0.4954	3 O
0.1603	37 H	-0.0584	26 N	0.1662	15 H	-0.4786	4 N
0.3064	38 H	0.2638	27 C	-1.0815	16 C	0.3384	5 H
-0.2513	39 C	0.1073	28 H	0.2130	17 C	-0.3309	6 C
0.1205	40 H	0.5177	29 C	0.4499	18 C	0.6140	7 C
0.1263	41 H	0.9662	30 C	0.6644	19 C	-0.0035	8 O
0.1251	42 H	-0.2698	31 C	0.1604	20 H	0.0279	9 C
-0.3049	43 N	-0.9877	32 C	-0.6270	21 C	0.1652	10 H
		-0.5304	33 C	0.1468	22 H	-0.3253	11 N

Table 10. Statistical parameters of experimental vs. theoretical ^{13}C chemical shifts

Correlation	Intercept	Slope	Method
0.9981	-3.540	1.056	**ISN**
0.9985	-2.215	1.051	**ISM**
0.9993	-2.333	1.042	**ISMT**

Figure Caption

Scheme 1. Preparation procedure of Schiff bases with general structure

Scheme 2. Suggested mass fragmentation of **ISN**

Fig. 1. ^{1}H NMR spectra of **ISM**

Fig. 2. Structure of **ISN**, **ISM** and **ISMT** with the numbering of the carbon atoms (which is only for ^{13}C NMR data assignments in Table 6)

Fig. 3. The optimized structure of **ISMT** within numbering of atoms obtained at B3LYP/6-311+G(d,p) level of theory.

Fig. 4. The atomic orbital compositions of the frontier molecular orbital of **ISMT**

Fig. 5. The Mulliken atomic charge distribution of **ISMT**

Fig. 6. Experimental values vs. theoretical ^{13}C NMR chemical shifts of **ISMT**

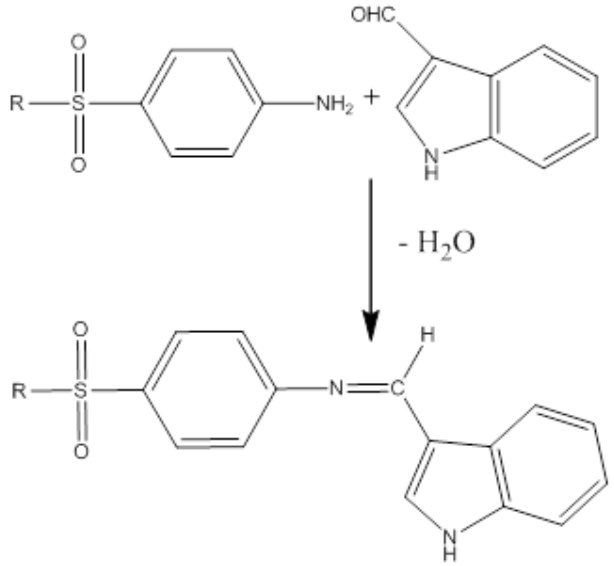

Comp.	R
ISN	—NH_2
ISPY	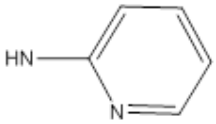
ISD	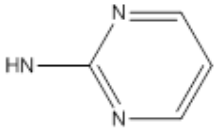
ISM	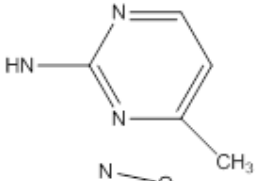
ISMT	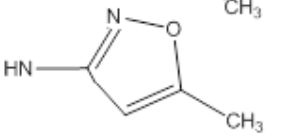
ISMP	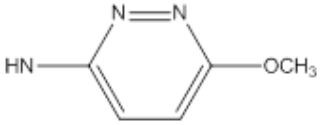
ISA	

Scheme 1. Preparation procedure of Schiff bases with general structure

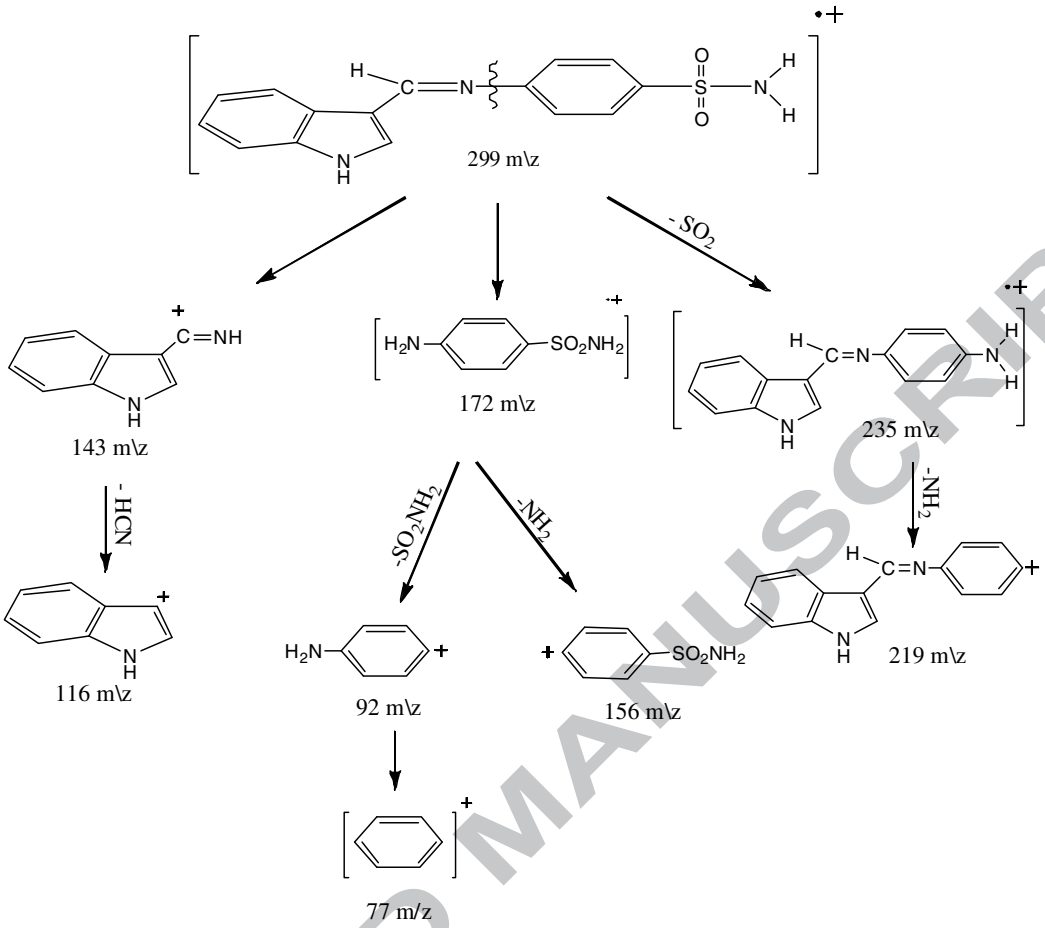

Scheme 2. Suggested mass fragmentation of **ISN**

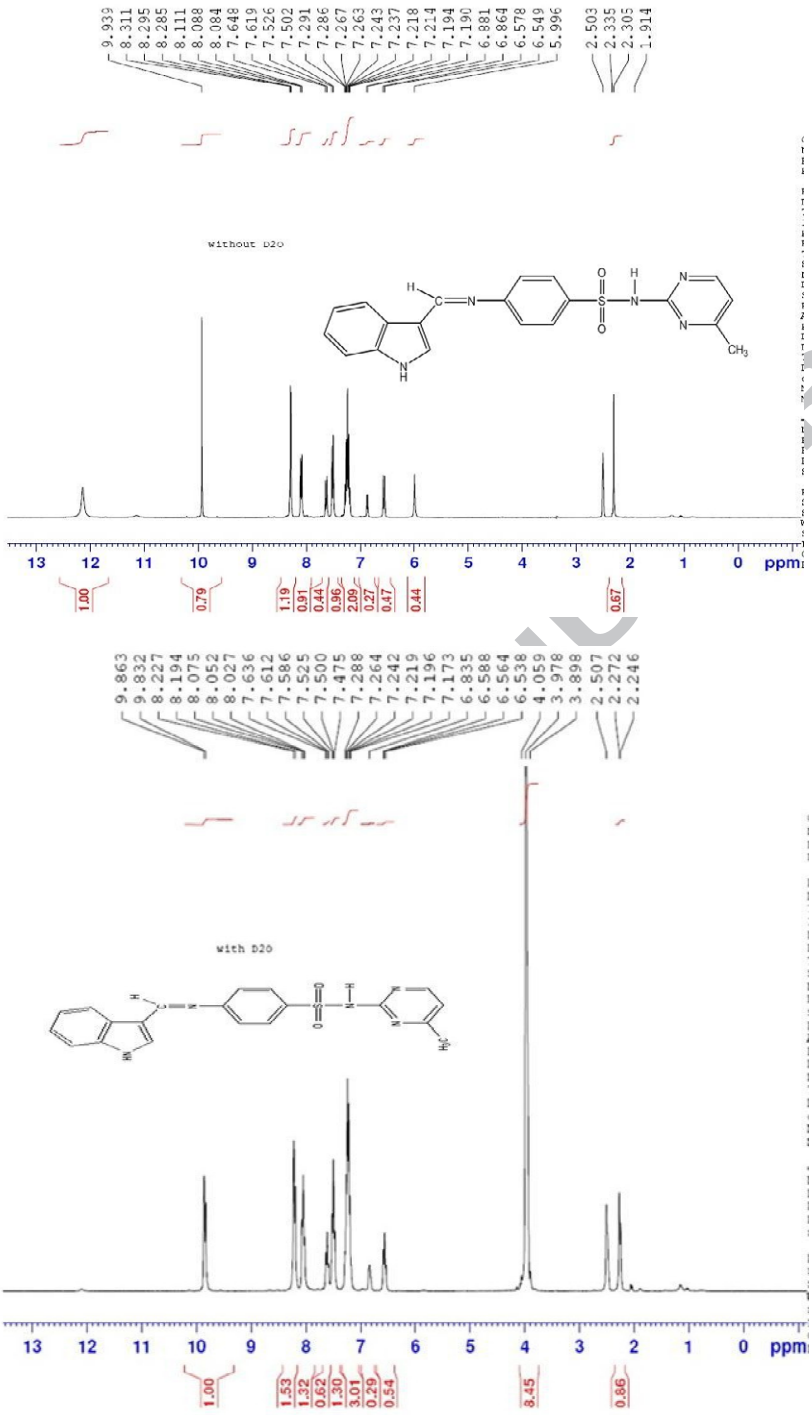

Fig. 1. ^{1}H NMR spectra of **ISM**

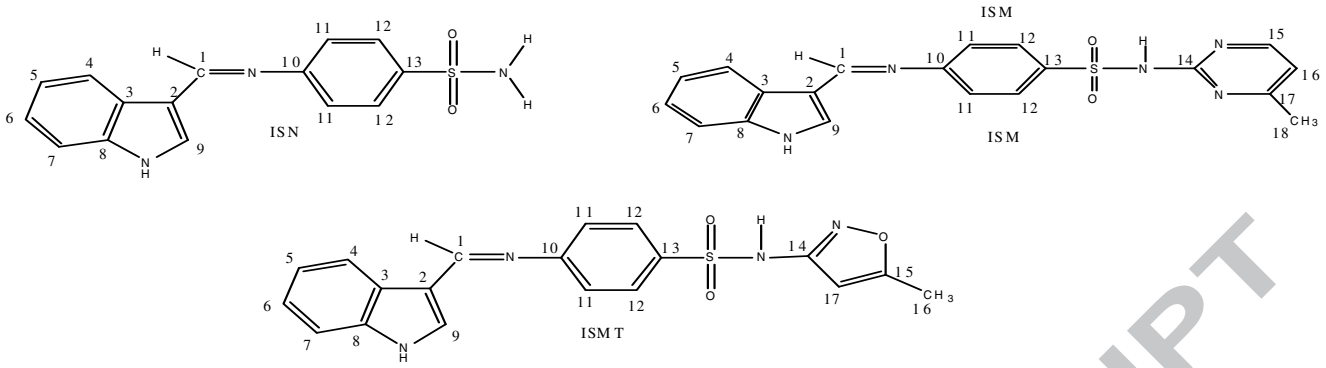

Fig. 2. Structure of **ISN**, **ISM** and **ISMT** with the numbering of the carbon atoms (which is only for ^{13}C NMR data assignments in Table 6)

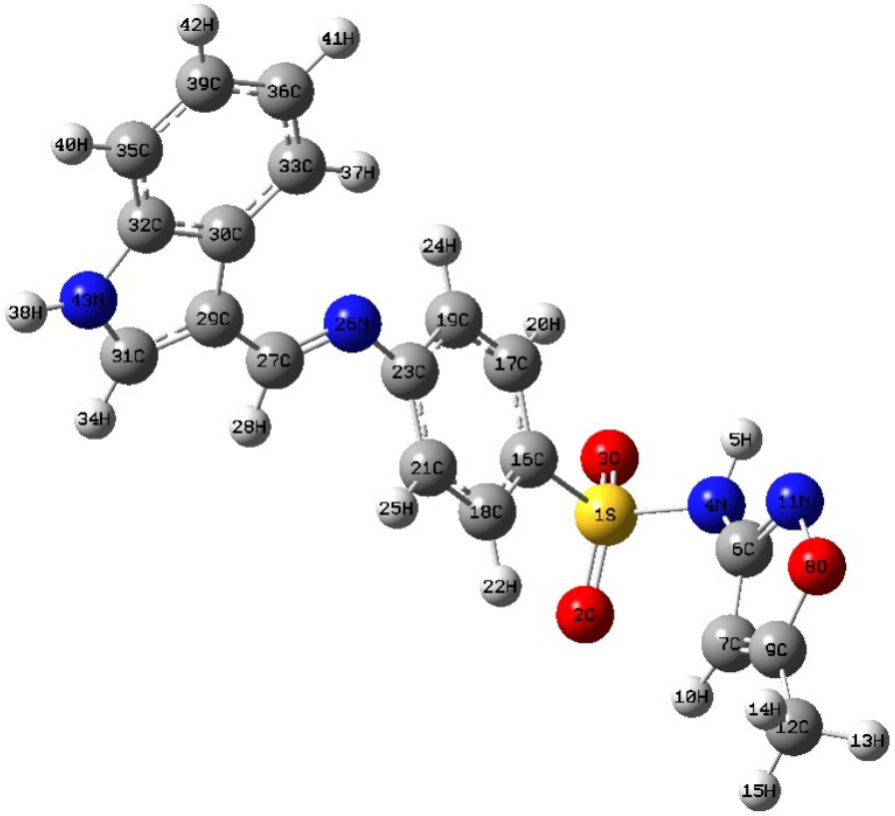

Fig. 3. The optimized structure of **ISMT** within numbering of atoms obtained at B3LYP/6-311+G(d,p) level of theory

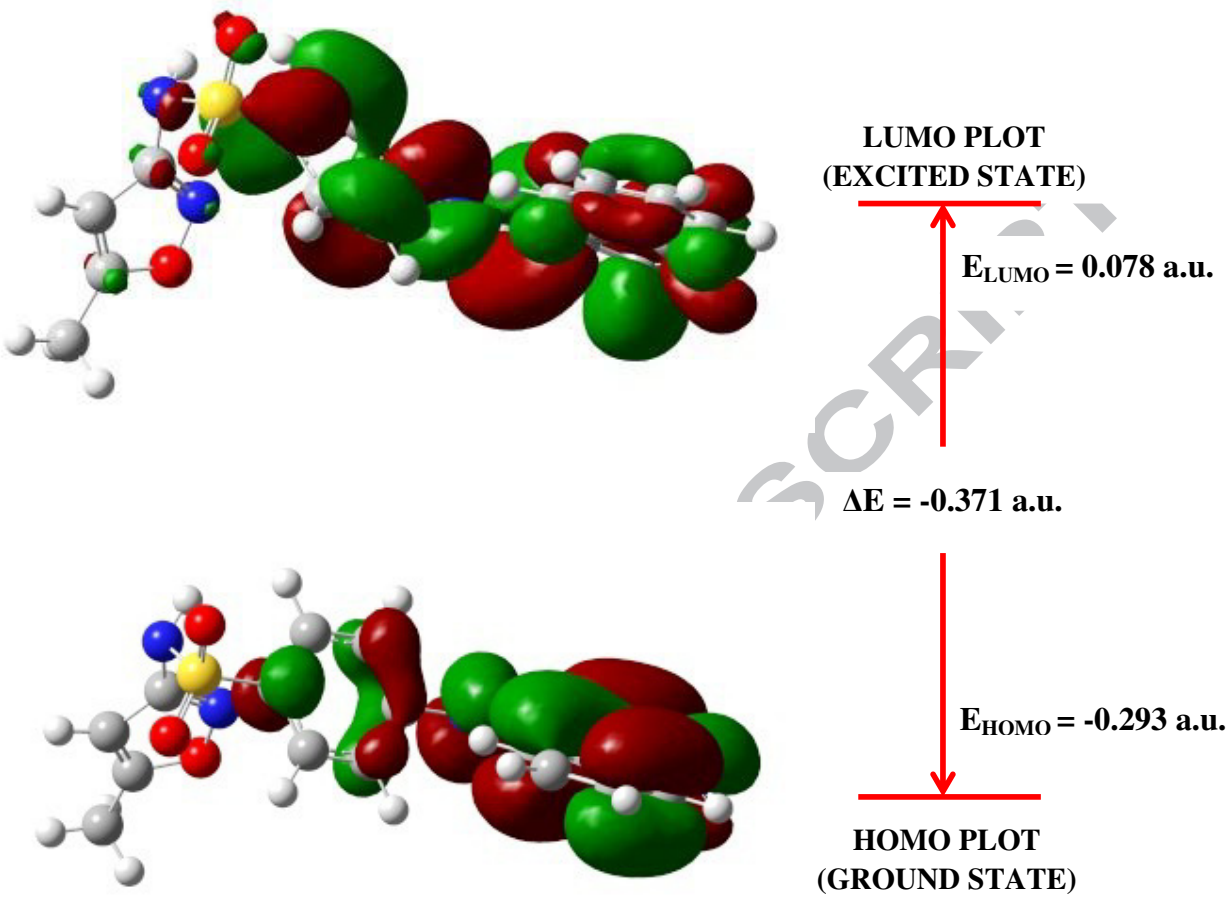

Fig. 4. The atomic orbital compositions of the frontier molecular orbital of **ISMT**

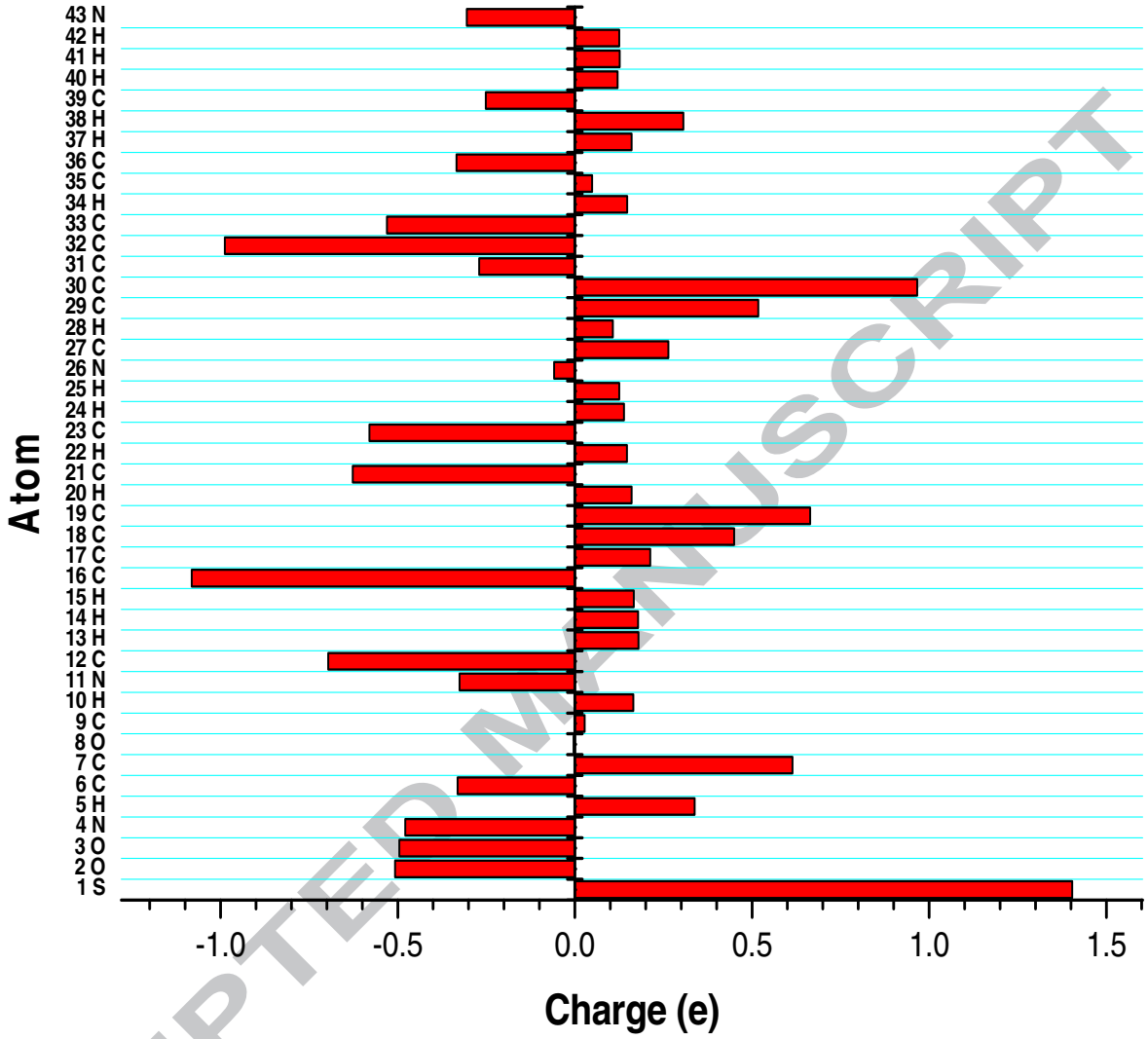

Fig. 5. The Mulliken atomic charge distribution of **ISMT**

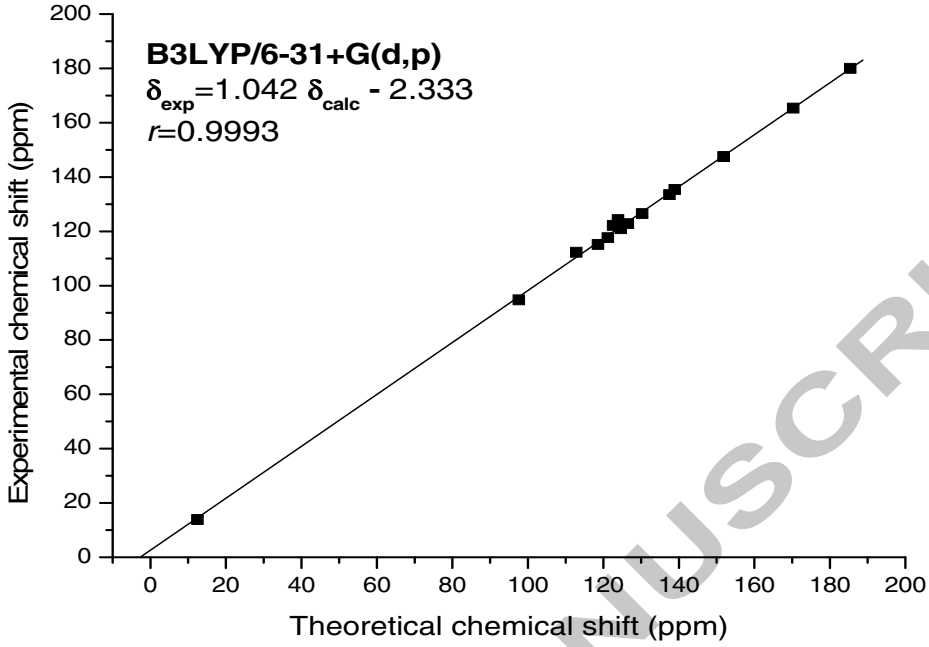

Fig. 6. Experimental values vs. theoretical ^{13}C NMR chemical shifts of **ISMT**

- A new series of Schiff bases were synthesized for the first time by the condensation of indole-3-carboxaldehyde with various sulfa drugs.
- The synthesized compounds were experimentally characterized using IR, ^{1}H NMR and ^{13}C NMR as well as mass spectroscopy.
- The theoretical calculations were performed using B3LYP as the more popular DFT methods at 6-31+G(d,p) level of theory.
- The structural properties as well as electronic analysis of studied compounds were reported.
- The calculated HOMO–LUMO transitions with frontier orbital gap and Mulliken atomic charges were presented.